Published online 21 January 2022

Nucleic Acids Research, 2022, Vol. 50, No. 3 ***1639–1649***
https://doi.org/10.1093/nar/gkab1260

The C nucleotide at the mature 5′ end of the *Escherichia coli* proline tRNAs is required for the RNase E cleavage specificity at the 3′ terminus as well as functionality

Bijoy K. Mohanty, Valerie Maples and Sidney R. Kushner*

Department of Genetics and Microbiology, University of Georgia, Athens, GA 30602, USA

Received October 06, 2021; Revised November 22, 2021; Editorial Decision December 06, 2021; Accepted December 09, 2021

ABSTRACT

Proline tRNA 3′-maturation in *Escherichia coli* occurs through a one-step RNase E endonucleolytic cleavage immediately after the CCA determinant. This processing pathway is distinct from the 3′-end maturation of the other tRNAs by avoiding the widespread use of 3′ → 5′ exonucleolytic processing, 3′-polyadenylation and subsequent degradation. Here, we show that the cytosine (C) at the mature 5′-terminus of the *proK* and *proL* tRNAs is required for both the RNase E cleavage immediately after the CCA determinant and their functionality. Thus, changing the C nucleotide at the mature 5′-terminus of the *proL* and *proK* tRNAs to the more common G nucleotide led to RNase E cleavages 1–4 nucleotides downstream of the CCA determinant. Furthermore, the 5′-modified mutant tRNAs required RNase T and RNase PH for their 3′-maturation and became substrates for polyadenylation and degradation. Strikingly, the aminoacylation of the 5′-modified proline tRNAs was blocked due to the change in the recognition element for prolyl-tRNA-synthetase. An analogous modification of the *pheV* 5′-mature terminus from G to C nucleotide did not support cell viability. This result provides additional support for the importance of first nucleotide of the mature tRNAs in their processing and functionality.

INTRODUCTION

The *Escherichia coli* genome contains 86 tRNA genes, which are transcribed either as polycistronic transcripts containing more than one tRNA, in association with mRNAs or rRNAs, or monocistronic transcripts containing a single tRNA (1). Each primary tRNA transcript undergoes extensive processing at both the 5′ and 3′ ends to generate functional tRNAs that can be aminoacylated. For many years, it was believed that all *E. coli* tRNAs are matured through a common processing pathway involving initial RNase E endonucleolytic cleavages to separate pre-tRNAs from the primary transcripts. Subsequently, the 5′ ends of the pre-tRNAs are matured by RNase P and the 3′ ends are matured by one or more 3′ → 5′ exonucleases.

Although some polycistronic tRNA transcripts (*argX hisR leuT proM* and *glyW cysT leuZ*) utilize the RNase E-based processing pathway (2,3), significant variations of this pathway have been identified (1). For example, the *valV valW* and *leuQ leuP leuV* primary transcripts do not utilize RNase E cleavages to generate the pre-tRNAs (4). Instead, RNase P cleaves at the mature 5′-end of each tRNA in the polycistronic transcript to generate the pre-tRNAs. The primary transcripts of the *secG leuU* and *metT* polycistronic operons only require RNase E for the removal of the Rho-independent transcription terminators. Subsequently, RNase P separates the pre-tRNAs by cleavages at the mature 5′ ends of the downstream species (5). For transcripts from complex operons, such as *lysT,* both RNase E and RNase P are involved in pre-tRNA separation and 5′ end maturation (6). In contrast, the primary transcript of *leuX* requires PNPase for the removal of its Rho-independent transcription terminator and is matured through an RNase E-independent pathway (7).

All of these tRNA processing pathways require one or more of the 3′ → 5′ exonucleases for the final 3′-end maturation. Though *E. coli* has multiple 3′ → 5′ exonucleases (RNase T, RNase PH, RNase D, RNase BN, RNase II and PNPase) that are capable of tRNA 3′-end maturation, RNase T and RNase PH carry out bulk of the final 3′ end processing (8). Consequently, the absence of 3′→ 5′ exonucleases (particularly RNase T and RNase PH) leads to widespread pre-tRNA polyadenylation by poly(A) polymerase I (PAP I), which modulates their processing and stability (8,9).

Escherichia coli contains three proline tRNAs which are encoded by *proK, proL* and *proM* genes. While both *proK*

*To whom correspondence should be addressed. Tel: +1 706 542 8000; Email: skushner@uga.edu

and *proL* are transcribed as monocistronic transcripts terminated with Rho-independent transcription terminators (10), *proM* is transcribed as part of the *argX hisR leuT proM* polycistronic transcript (2,3). Interestingly, unlike the majority of the tRNAs, the *proK, proL* and *proM* transcripts are matured at their 3′-ends by a single RNase E cleavage immediately downstream of the CCA determinant, thus not requiring any 3′→ 5′ exonucleolytic activity (10). As a result, the proline tRNAs are resistant to polyadenylation in both wild-type and 3′→ 5′ exonuclease deficient strains (8). In addition to the three proline tRNAs, the *metV, metW, metY* and *metZ* initiator tRNAs are also not affected by the absence of 3′→ 5′ exonucleases (8) and may be subject to similar one-step 3′-end maturation.

Presently, our understanding of the RNase E cleavage specificity is based on studies, which suggested that the ribonuclease preferentially cleaves within AU-rich sequence elements (AUE) (11–14). In fact, AUE regions have been shown to be conserved downstream of many tRNAs in *E. coli* (15). Furthermore, RNase E cleavage at an AUE sequence downstream of many tRNA CCA termini leaves 1–3 nt, thereby requiring at least one of the 3′ → 5′ exonucleases, usually RNase T and/or RNase PH, to complete the final 3′-end maturation. Surprisingly, despite having AUE sequences downstream of their CCA determinants that are very similar to other tRNAs, RNase E cleavage specificity has been significantly altered for the proline tRNAs. For example, the *proK, pheU* and *leuU* tRNAs have very similar AUE sequences downstream of their CCA determinants (10), but RNase E cleaves immediately after the CCA for *proK* (10), whereas it cleaves 1–2 nts downstream of the CCA for *pheU* and *leuU* (5,16). Similarly, both *proL* and *leuX* contain almost identical AUE sequences downstream of the CCA. However, while *proL* is cleaved by RNase E immediately after the CCA, the *leuX* tRNA is not actually an RNase E substrate (7,10).

In this report, we have investigated what makes the proline tRNAs distinct from other tRNAs in terms of their RNase E cleavage specificity. Earlier, we showed that 79/86 tRNAs in *E. coli* have either the G (67 tRNAs), U (8 tRNAs) or A (4 tRNAs) nucleotide at their mature 5′ termini (10). In contrast, the proline tRNAs encoded by *proK, proL* and *proM* and the initiator methionine (iMet) tRNAs encoded by *metZ, metW, metV* and *metY* have a 5′ C residue. However, unlike all other tRNAs including the proline tRNAs where the first residue at the mature 5′-end forms a Watson-Crick base pair with a complementary nucleotide at position 72 (Figure 1), the first residue of all the iMet-tRNAs is mismatched. Furthermore, a sequence analysis of genomic tRNAs from 1546 bacterial species has identified G as the primary first nucleotide of a tRNA (∼85% of the time) followed by U (∼6%), C (∼6%) and A (∼3%). The G1-C72 Watson-Crick base pair accounts for ∼81% of bacterial tRNAs whereas C1-G72 appears only in ∼5% of tRNAs which includes all the proline tRNAs (17). Here we show that the C residue at the 5′ mature end of the *proK* and *proL* tRNAs is required for RNase E cleavage immediately after the CCA determinant. Thus, changing the 5′ C to G in the *proL* and *proK* tRNAs led to the RNase E cleavage at 1–4 nts downstream of CCA instead of immediately after

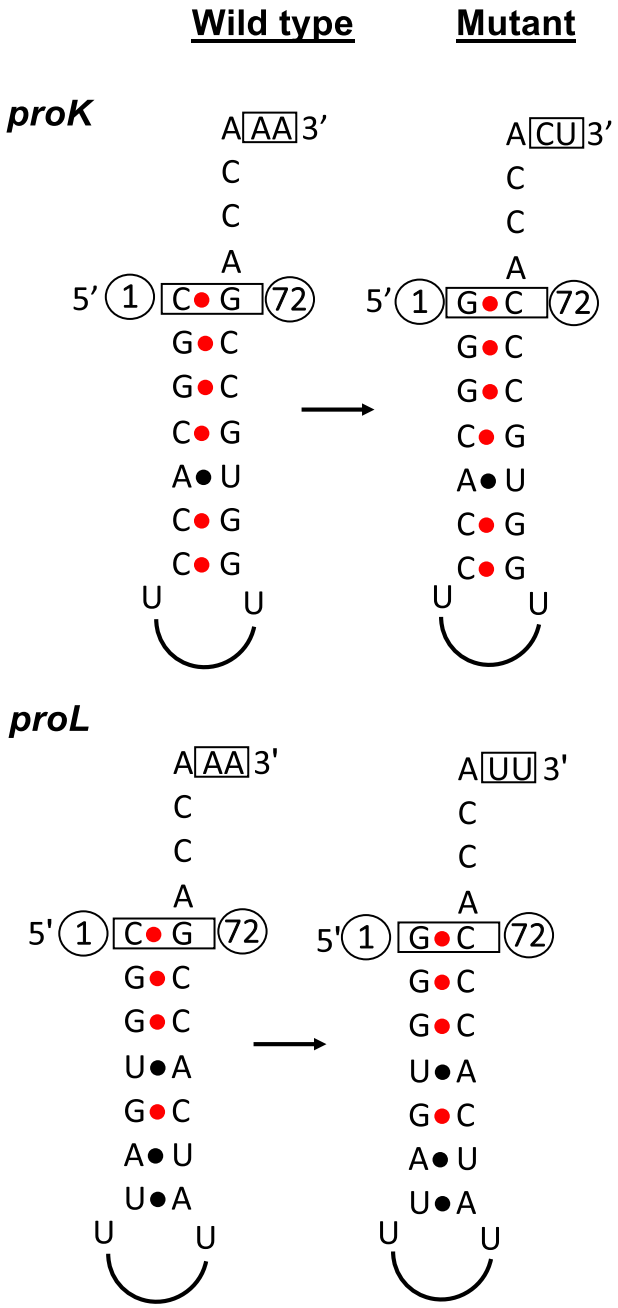

Figure 1. Graphical presentation of the *proK* and *proL* tRNAs showing the base pairings in the acceptor stem. The nucleotides which were modified in the wild-type tRNA sequences to obtain the mutant tRNA are shown in a box. C1/G72 base pairing in the acceptor stems of *proK* and *proL* tRNAs was changed to G1/C72. AA nucleotides downstream of *proK* CCA was changed to CU to mimic *cysT* CCA downstream sequence. AA nucleotides downstream of *proL* CCA was changed to UU to mimic *hisR* CCA downstream sequence. The nucleotide numbers are shown in circles.

the CCA. However, changing the 3′ downstream sequences following the CCA determinant in the *proL* and *proK* tRNAs to that of either *hisR* or *cysT* had no significant effect on their 3′ end processing. Furthermore, the change of the 5′ nucleotide to the much more common G nucleotide also resulted in a tRNA that could not be aminoacylated. The

importance of the first nucleotide at the mature 5′ end is discussed.

MATERIALS AND METHODS

Bacterial strains and plasmids

The bacterial strains and plasmids used in this study are listed in Supplementary Table S1. All the *E. coli* strains were constructed in SK10153 (*thyA715*), a MG1693 derivative that contains a wild-type *rph* gene (8). The chromosomal copies of *proL* (7 nts upstream of the mature 5′ terminus and 42 nts downstream of the CCA), *proK* (67 nts upstream of the mature 5′ terminus and 34 nts downstream of the CCA), *pheU* (94 nts upstream of the mature 5′ terminus to 41 nt downstream of the CCA) and *pheV* (137 nt upstream of the mature 5′ terminus to 134 nt downstream of the CCA) coding sequences were deleted using the method of Datsenko *et al.* (18). Originally constructed in BW25113, all the deletion alleles were moved into the SK10153 genetic background using P1-mediated transduction to obtain SK5976 (*ΔproK*::Km^R-FRT *thyA715*), SK5096 (*ΔproL*::Apr^R-FRT *thyA715*), SK4235 (*ΔpheV*::Apr^R-FRT *thyA715*) and SK4242 (*ΔpheU*::Cm^R-FRT *thyA715*).

The *ΔpheV*::Apr^R-FRT allele was moved into the strain containing *ΔpheU*::Cm^R-FRT by P1 transduction in the presence of a low copy number plasmid expressing the wild-type *pheV* (pVMK204, *pheV*/Tet^R). Subsequently, the FRT-flanked antibiotic resistance genes (Km^R, Apr^R and Cm^R) used to mark the various deleted genes (proK, *proL*, *pheU* and *pheV*) were removed using the FLP helper plasmid (pCP20) as described previously (18) to construct SK5999 (*ΔproK thyA715*), SK10911 (*ΔproL thyA715*) and SK4244 (*ΔpheV ΔpheU*/pVMK204/Tc^R). The additional strains listed in Supplementary Table S1 were made using either plasmid transformation or P1-mediated transduction.

Construction of plasmids expressing wild-type and mutant tRNA^{Pro} and tRNA^{PheV}

All plasmids expressing either the wild-type or mutant tRNA genes were constructed using the low copy number plasmid pWKS130 (Km^R) (6–8 copies/cell) (19). The coding sequences for *proK* (44 nt upstream of the mature 5′ terminus and 41 nt downstream of CCA), *proL* (47 nt upstream of the mature 5′ terminus and 47 nt downstream of CCA) and *pheV* (58 nt upstream of the mature 5′ terminus and 61 nt downstream of CCA) were amplified employing a high-fidelity DNA polymerase (Q5, NEB) and gene specific upstream and downstream primers containing the desired restriction sites for cloning. The amplified PCR products contained the tRNA coding sequences under their own promoter and terminator sequences. The 5′ and 3′ sequences were modified by introducing the desired nucleotides into the PCR primers in order to generate mutant *proK, proL* and *pheV* tRNAs. All PCR fragments were cloned into pWKS130 (19) either at the *Sac*II-*Xba*I (*proK* and *proL*) or *Pst*I-*Sal*I (*pheV*) sites. All the plasmids expressing the wild-type and the mutant *proK, proL* or *pheV* genes were sequenced to confirm the nucleotide changes and are listed in Table 1 and Supplementary Table S1.

Table 1. Various *proK, proL* and *pheV* plasmids used in the study. The *proK*, *proL* and *pheV* coding sequences without or with the indicated modifications were cloned with their native promoters and terminators in pWKS130, a 6–8 copy vector (19)

Plasmids	Genotype	Description
pBMK72	$proK^{WT}$	Wild-type *proK* coding sequences.
pBMK73	$proK^{3M}$	3′ sequences downstream of CCA were changed from AA → CU (same as *cysT*).
pBMK74	$proK^{5M}$	C/G base pair at the 5′-mature terminus was changed to G/C base pair.
pBMK75	$proK^{5M+3M}$	The 5′-mature termini and 3′ downstream sequences of CCA were changed as described for pBMK74 and pBMK73, respectively.
pBMK77	$proL^{WT}$	Wild-type *proL* coding sequences.
pBMK78	$proL^{5M}$	C/G base pair at the 5′-mature terminus was changed to G/C base pair.
pBMK80	$proL^{3M}$	3′ sequences downstream of CCA were changed from AA → UU (same as *hisR*).
pBMK81	$proL^{5M+3M}$	The 5′-mature termini and 3′ downstream sequences of CCA were changed as described for pBMK78 and pBMK80, respectively.
pVMK208	$pheV^{WT}$	Wild-type *pheV* coding sequences.
pVMK210	$pheV^{3M}$	3′ sequences downstream of CCA were changed from CUAA → AAUU (same as *proK*).
pVMK212	$pheV^{5M+3M}$	The 5′-mature termini and 3′ downstream sequences of CCA were changed as described for pVMK214 and pVMK210, respectively.
pVMK214	$pheV^{5M}$	G/C base pair at the 5′-mature terminus was changed to C/G base pair.

Growth of bacterial strains and plasmid displacement

The bacterial strains were grown in a water bath shaker at 37°C in Luria broth supplemented with thymine (50 μg/ml). When appropriate, ampicillin (50 μg/ml), apramycin (50 μg/ml), chloramphenicol (20 μg/ml), kanamycin (25 μg/ml) and/or tetracycline (25 μg/ml) were added to the culture medium. Bacterial growth was monitored using a Klett-Summerson Colorimeter (No.42 Green filter).

To carry out plasmid displacements, a *ΔpheV ΔpheU* recipient strain carrying a covering plasmid with the wild-type *pheV* gene (pVMK208/$pheV^{WT}$) (Supplementary Table S1) was chemically transformed with a plasmid carrying a modified *pheV* tRNA sequence and a different drug resistance marker than the resident plasmid. The transformants were selected at 37°C based on the drug marker carried on the incoming plasmid. Individual transformants were then grown for 3 days in the presence of the drug carried on the incoming plasmid. Every 12 h, the culture was diluted (1:50) in fresh medium. Subsequently, the loss of the resident plasmid was determined by replica plating 50–100 individual colonies.

RNA isolation and northern blot analysis

Total steady-state RNA isolation and northern blot analyses were performed as described previously (20). All RNA samples were treated with DNase I to remove any residual DNA contamination as described before (20).

RT-PCR cloning and sequencing of 5′-3′ self-ligated transcripts

The analyses of the 5′ and 3′-ends of the proline tRNAs were carried out by cloning and sequencing the reverse transcription PCR products derived from 5′-3′ self-ligated circular *proK* and *proL* tRNAs as described previously (10).

Determination of *in vivo* aminoacylation

All the bacterial strains were grown to 50 Klett units above background (mid exponential phase) when the cells were growing exponentially (∼1–1.1 × 10^8 cells/ml) at 37ºC. Total RNA from 15 ml of culture was isolated under acidic conditions to preserve tRNA aminoacylation as described previously (8,21). All the RNA samples were quantified using a Nanodrop (ND2000c) apparatus. Half of each RNA sample was deacylated by treating with 0.5 M Tris (pH 9.0) for 30 minutes at 37°C. Subsequently, both untreated and Tris-treated samples (2.5 μg each) were separated on 6.5% (w/v) acid-urea polyacrylamide gels run in the cold room and transferred to a positively charged nylon membrane (Nytran® SPC, Whatman®) as described previously (8). The membranes were subsequently probed with ^{32}P-labelled gene specific oligonucleotides (Supplementary Table S2).

Oligonucleotide probes

Although the three mature proline tRNAs have highly homologous sequences, the probes used here to successfully distinguish the *proL, proK* and *proM* tRNAs have been previously reported (10). All oligonucleotides used in this study are listed in Supplementary Table S2.

RESULTS

Construction of modified *proL and proK* tRNAs

We have noted previously that the three proline tRNAs (*proK, proL* and *proM*) contain a cytosine (C) nucleotide at their mature 5′ terminus (Figure 1) compared to all the other tRNAs that have either G, A or U. Since the proline tRNA 3′-ends are matured by a single RNase E cleavage in contrast to all other tRNAs, we hypothesized that the C residue at the mature 5′ end of proline tRNAs might have a role in the RNase E cleavage immediately downstream of the CCA determinant.

Initially, we cloned the wild-type coding sequences of *proL* ($proL^{WT}$) and *proK* ($proK^{WT}$) in pWKS130 (6–8 copy number) to generate the pBMK77 ($proL^{WT}$) and pBMK72 ($proK^{WT}$) plasmids, respectively (Table 1). Both genes were transcribed from their respective native promoters and retained the downstream sequences containing their Rho-independent transcription terminators. Since G is the most common first nucleotide at the mature 5′ end of majority of *E. coli* tRNAs (67/86), which pairs with C72 residue as part of the acceptor stem, we replaced the C1/G72 base pair with a G1/C72 base pair at the mature 5′ end in the *proK* and *proL* coding sequences. Thus, the base pairings in the acceptor stem in the mutant tRNAs remain unchanged (Figure 1). The 5′ modified (G1/C72) proline coding sequences were cloned to construct pBMK74 ($proK^{5M}$) and pBMK78 ($proL^{5M}$), respectively.

To determine if the nucleotides downstream of the CCA determinant played any role in RNase E cleavage specificity, we also introduced nucleotide changes immediately downstream of the CCA trinucleotide (3′ modified) to mimic either the *cysT* (in $proK^{3M}$) or *hisR* (in $proL^{3M}$) tRNAs (Figure 1), since RNase E cleaves these two tRNAs 1–2 nt downstream of their CCA determinants (3). The resulting plasmids were pBMK73 ($proK^{3M}$) and pBMK80 ($proL^{3M}$), respectively (Table 1). In addition, two additional variants of both the *proK* and *proL* tRNAs were constructed in which both the 5′ and 3′ modifications were combined to construct pBMK75 ($proK^{5M+3M}$) and pBMK81 ($proL^{5M+3M}$), respectively (Table 1).

Deletion of either *proL* or *proK* or both genes has no effect on the growth and viability of *E. coli*

While *proL* and *proK* are transcribed as monocistronic genes (10), *proM* is the last gene in the *argX hisR leuT proM* polycistronic operon (2,3). To clearly distinguish the proline tRNAs expressed from the extrachromosomal plasmids described above from genomically encoded wild-type tRNAs, the chromosomal copies of the *proL* and *proK* genes were individually deleted as described in the Materials and Methods section. Northern analysis confirmed the absence of genomic *proL* and *proK* transcripts (Figure 2B–D, lane 1). The generation times of the *ΔproL* and *ΔproK* single mutants as well as a *ΔproL ΔproK* double mutant were comparable to the wild-type control when grown on either Luria agar or in Luria broth (Supplementary Figure S1). However, it was not possible to delete *proM* using the same method, suggesting that *proM* is essential and sufficient for maintaining growth and cell viability.

Extrachromosomal expression of the *proL* and *proK* tRNAs resulted in differential effects on their steady-state levels

The effects of 5′ and 3′ modifications to the proline tRNAs were studied by expressing the modified proline coding sequences in the *ΔproL* and *ΔproK* genetic backgrounds from the extrachromosomal plasmids as described in Table 1. There were no significant growth differences between the wild-type and the strains expressing the proline coding sequences from plasmids (data not shown). Subsequently, we determined the steady-state level of each modified transcript compared to the chromosomally expressed proline transcripts using northern blot analyses. The steady-state levels of $proL^{WT}$ and $proL^{3M}$ tRNAs increased ∼5 ± 1-fold compared to genomic *proL* expression in the wild-type control (Figure 2B, lanes 2, 3 and 5). These results were consistent with the copy number of the vector pWKS130 (6–8 copies per cell) (19). Surprisingly, the steady-state levels of the $proL^{5M}$ and $proL^{5M+3M}$ tRNAs were reduced almost 5-fold, since their expression was identical to the genomic *proL* expression in the wild-type control (Figure 2B, lanes 2, 4 and 6), suggesting an effect of the 5′ and/or 3′ modifications.

A very different expression pattern was observed with the *proK* tRNAs. In the first place, the steady-state levels of both wild-type ($proK^{WT}$) and the mutant ($proK^{3M}$,

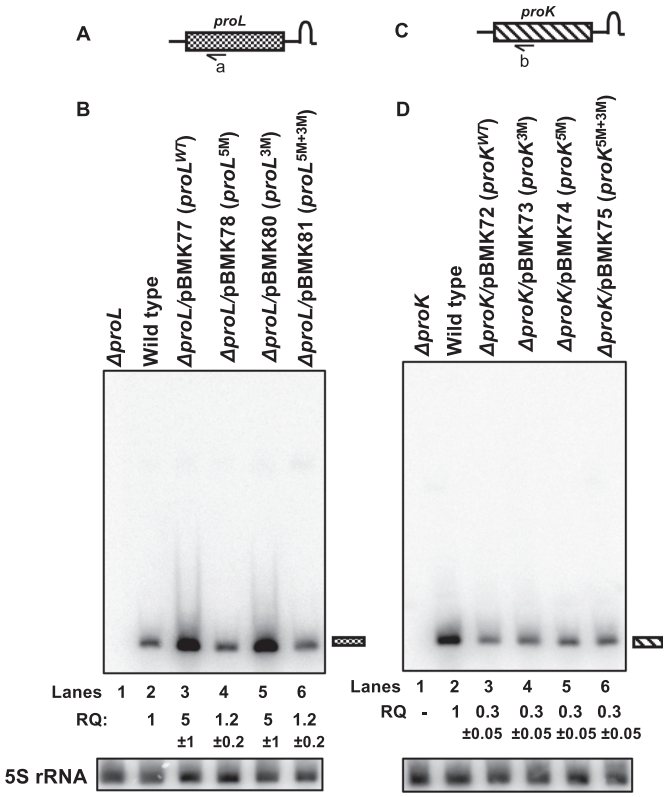

Figure 2. Northern blot analyses of the processing of *proL* and *proK* tRNAs expressed from various plasmids. Total steady-state RNA (10 μg/lane) isolated from exponentially growing cultures at 37°C was separated on a 6% (w/v) polyacrylamide/ 8 M urea gel, transferred to nylon membrane and probed with transcript specific ^{32}P-labeled oligonucleotide probes. Schematic presentation of (**A**) *proL* and (**C**) *proK* genes (not drawn to scale) in the genome. Relative positions of the oligonucleotide probes (a: PROL-2 and b: PROK-2, Supplementary Table S2) used in the northern blot analyses are shown below the cartoon. Northern blots of (**B**) *proL* tRNA probed with probe a and (**D**) *proK* tRNA probed with probe b. The genotypes of the strains used are indicated at the top of each blot. The position of the mature tRNA is indicated to the right of the blots. The northern blot of 5S rRNA used as a loading control is shown below each blot. Relative quantity (RQ) of mature tRNA in each strain represent an average of three independent analyses. RQ was calculated based on the pixel counts in each strain and the wild-type pixel count was considered as 1.

proK^{5M} and *proK*$^{5M+3M}$) tRNAs were reduced over 3-fold compared to the genomic *proK* tRNA level (Figure 2D, lanes 2–6), even though all plasmids were 6–8 copy numbers similar to pBMK77 (*proL*^{WT}). Surprisingly, *proK*^{5M} and *proK*$^{5M+3M}$ sequences in *ΔproK*/pBMK74 (*proK*^{5M}) and *ΔproK*/pBMK75 (*proK*$^{5M+3M}$) strains, respectively, picked up a spontaneous mutation (deletion of G) in the -35 region (TTGACG to TTACG) of the promoter (10) (Supplementary Figure S2), when allowed to grow longer periods on solid medium before growing in the liquid medium. This mutation either significantly reduced or shut off the transcription of the plasmid encoded *proK* gene. Furthermore, the mutation frequency appeared to be higher in the *ΔproK*/pBMK75 (*proK*$^{5M+3M}$) strain compared to the *ΔproK*/pBMK74 (*proK*^{5M}) strain. Accordingly, all expression studies described here were carried out using fresh transformants.

We have shown previously that the full-length proline transcripts containing their Rho-independent transcription terminators accumulate in the absence of either RNase E alone (*proK* and *proM*) or both RNase E and PNPase (*proL*) (10). Since we did not detect any full-length proline transcripts in the northern blots shown in Figure 2B–D, suggesting the almost complete removal of the Rho-independent transcription terminators, we wanted to confirm that RNase E was indeed removing the terminators from the mutant proline transcripts. Accordingly, all the plasmids were expressed in the appropriate *rne-1 ΔproK* and *rne-1Δpnp ΔproL* multiple mutants at the nonpermissive temperature (44°C) in order to inactivate RNase E. As expected, the full-length transcripts of *proL* (Supplementary Figure S3A, lanes 3–6) and *proK* (Supplementary Figure S3B, lanes 3–6) were observed in the absence of RNase E, which demonstrated the requirement of RNase E for the terminator removal for all the proline tRNA variants.

Together, above data suggested that the steady-state levels of both the *proL* and *proK* tRNAs were significantly affected by changing the 5′ terminal nucleotide from a C to a G (Figure 2B, D). Although 3′ modification alone in both tRNAs had no significant effect in their expression, the combined 5′ and 3′ modifications in *proK* enhanced its susceptibility to mutation.

5′ modification of proL *and* proK *transcripts changed the 3′ processing sites downstream of the CCA determinants.* To determine the *in vivo* cleavage sites in the mutant proline tRNAs, the RNA used in the northern blot analyses (Figure 2B, D) was employed to generate cDNAs from 5′ to 3′ self-ligated transcripts, which were sequenced to identify both 5′ and 3′ termini as described previously (10). The sequences of 32 independent *proL*^{WT} cDNAs (32/32) showed that all of them were processed at their mature 5′ and 3′ ends (Figure 3A), which was consistent with our previous report (10). Changing the sequences downstream of *proL* tRNA CCA to those associated with the *hisR* tRNA (AA to UU, Figure 1) did not change the 3′ processing of the *proL*^{3M} transcripts significantly, since ∼92% of the sequenced cDNAs (22/24) showed that the tRNAs were processed exactly at the 3′-end (Figure 3B). The presence of UU nucleotides downstream of CCA in the remaining ∼8% of the tRNAs (2/24 cDNAs) confirmed that the pre-tRNAs were transcribed with the 3′ modification. However, ∼17% of *proL*^{3M} tRNA (4/24 cDNAs) had immature 5′-ends.

The most striking changes in the processing of the *proL* transcripts were observed for both the 5′ (*proL*^{5M}) as well as 5′ plus 3′ (*proL*$^{5M+3M}$) modified transcripts. While only ∼30% of the *proL*^{5M} tRNAs (9/30 cDNAs) had mature 3′ ends, ∼57% of tRNAs (17/30 cDNAs) were cleaved starting at 2 nt downstream of the CCA determinant (Figure 3C). The 5′ maturation catalyzed by RNase P also appeared to be inefficient, since ∼40% of the tRNAs (12/30 cDNAs) were immature at the 5′-end. Similarly, only ∼30% of *proL*$^{5M+3M}$ tRNAs (8/27 cDNAs) had mature 3′ ends, while ∼59% of *proL*$^{5M+3M}$ tRNAs (16/27 cDNAs) were cleaved starting at 2 nt downstream of the CCA determinant (Figure 3D). The 5′ maturation was also impaired with ∼44% of the tRNAs (12/27 cDNAs) being immature at the 5′-end.

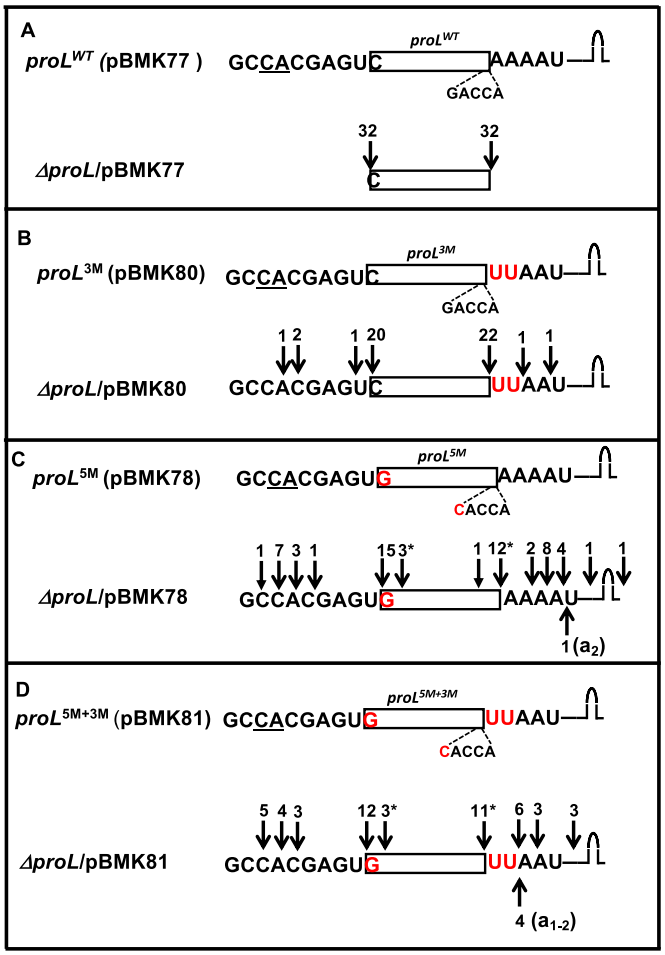

Figure 3. (**A**–**D**) Determination of 5′ and 3′ termini of *proL* tRNAs expressed from various plasmids in the *ΔproL* strain. The cDNAs were obtained by RT-PCR cloning of 5′-3′ self-ligated transcripts. The sequencing data from each strain are presented in a separate box. The cartoon at the top of each box is a graphic representation of the cloned *proL* genes with the coding sequences upstream and downstream of the 5′ and 3′ mature ends, respectively. The 5′ modification of C/G base pair to G/C and the 3′ modification of AA→UU are indicated in red. Transcription start sites are underlined (10). Each downward arrow represents either 5′ or 3′ ends (total number indicated at the top) as determined by sequence analysis. Some cDNAs were truncated either at the 5′ ends (*) or at the 3′ ends (downward solid arrow). Each upward arrow represents a 3′ end with untemplated A nucleotides (in parenthesis).

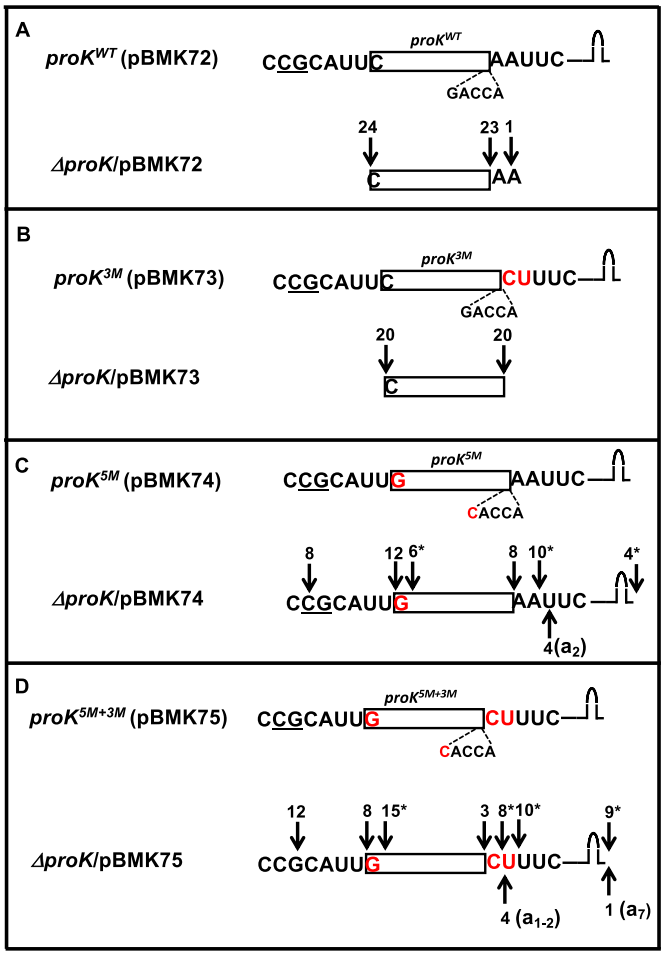

Figure 4. (**A**–**D**) Determination of 5′ and 3′ termini of *proK* tRNAs expressed from various plasmids in the *ΔproK* strain. The cDNAs were obtained by RT-PCR cloning of 5′-3′ self-ligated transcripts. The sequencing data from each strain are presented in a separate box. The cartoon at the top of each box is a graphic representation of the cloned *proK* genes with the coding sequences upstream and downstream of the 5′ and 3′ mature ends, respectively. The 5′ modification of C/G base pair to G/C and the 3′ modification of AA→CU are indicated in red. Transcription start sites are underlined (10). Each downward arrow represents either 5′ or 3′ ends (total number indicated at the top) as determined by sequence analysis. Some cDNAs were truncated at the 5′ ends (*). Each upward arrow represents a 3′ end with untemplated A nucleotides (in parenthesis).

Analyses of *proK* cDNAs showed that ∼96% (23/24 cDNAs) of the $proK^{WT}$ tRNAs were processed at their mature 3′ ends and all 24 tRNAs had mature 5′-ends (Figure 4A), which was consistent with our previous report (10). Similarly, all the sequenced $proK^{3M}$ tRNA (20/20 cDNAs) had both 5′ and 3′ mature ends (Figure 4B), suggesting that changing the nucleotides 3′ downstream of *proK* CCA from AA to CU (same as *cysT*) had no effect on the maturation of *proK* tRNA. In contrast, only ∼31% of $proK^{5M}$ tRNAs (8/26 cDNAs) had mature 3′ ends and ∼69% of the tRNAs (18/26 cDNAs) had unprocessed downstream sequences of at least two nucleotides (Figure 4C). Only ∼9% of $proK^{5M+3M}$ tRNAs (3/35 cDNAs) had mature 3′ ends, while ∼91% of the tRNAs (32/35 cDNAs) had at least one unprocessed nucleotide downstream of CCA (Figure 4D). In addition, ∼31% of $proK^{5M}$ tRNA (8/26 cDNAs) and ∼34% of the $proK^{5M+3M}$ tRNAs (12/35 cDNAs), also had 5′ unprocessed nucleotides. Surprisingly, the Rho-independent transcription terminators of ∼15–25% of both $proK^{5M}$ (4/26 cDNAs) and $proK^{5M+3M}$ tRNAs (9/35 cDNAs) were also not processed, suggesting a significant reduction in RNase E processing efficiency of the mutant *proK* transcripts.

Overall, the sequencing data showed that the amount of mature $proL^{3M}$ tRNAs was similar to $proL^{WT}$ and that the level of mature $proK^{3M}$ tRNAs was similar to $proK^{WT}$ (Figure 5A). However, the level of mature $proL^{5M}$ and $proL^{5M+3M}$ tRNAs decreased ∼2.5–3.0-fold compared to the $proL^{WT}$. In contrast, the level of mature $proK^{5M}$ decreased ∼4-fold and $proK^{5M+3M}$ tRNAs decreased ∼11-fold

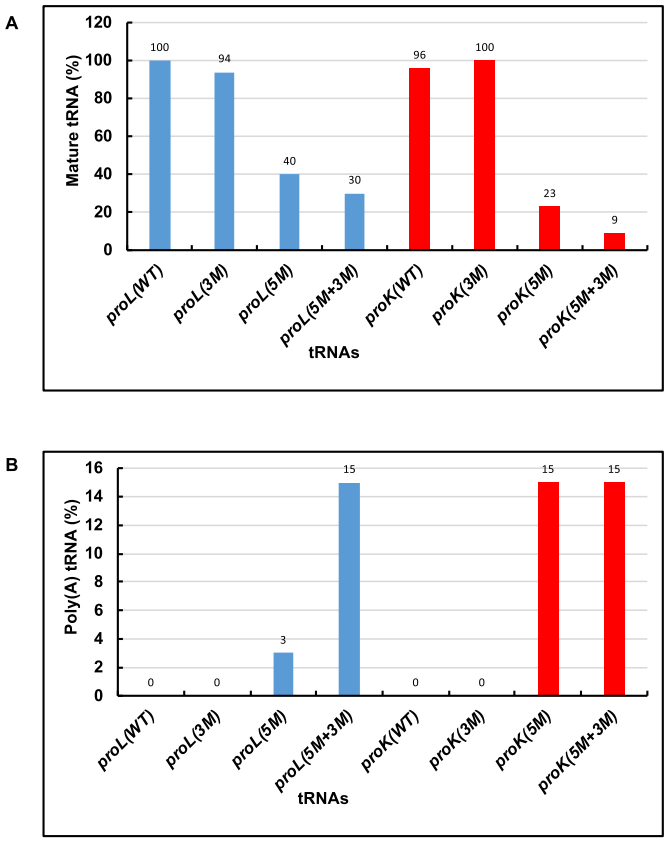

Figure 5. Mature tRNA (**A**) and polyadenylated pre-tRNA (**B**) levels in various strains containing different proline tRNAs as obtained from the cDNA cloning and sequencing. The percentage of the mature tRNA (both the 5′ and 3′ ends were matured) levels was calculated based on number of cDNAs corresponding to the mature tRNA (MT) sequenced out of total number of cDNAs corresponding to all tRNAs (AT) sequenced and shown in Figures 3 and 4. $proL^{WT}$: 22 MT/22 AT, $proL^{3M}$: 20 MT/22 AT, $proL^{5M}$: 12 MT/30 AT, $proL^{5M+3M}$: 8 MT/27 AT, $proK^{WT}$: 23 MT/24 AT, $proK^{3M}$: 20 MT/20 AT, $proK^{5M}$: 6 MT/26 AT and $proK^{5M+3M}$: 3 MT/35 AT. The percentage of polyadenylated pre-tRNA levels was calculated based on number of cDNAs corresponding to the pre-tRNA (PT) sequenced out of total number of cDNAs corresponding to all tRNAs (AT) sequenced and shown in Figures 3 and 4. $proL^{WT}$: 0 PT/22 AT, $proL^{3M}$: 0 PT/22 AT, $proL^{5M}$: 1 PT/30 AT, $proL^{5M+3M}$: 4 PT/27 AT, $proK^{WT}$: 0 PT/24 AT, $proK^{3M}$: 0 PT/20 AT, $proK^{5M}$: 4 PT/26 AT and $proK^{5M+3M}$: 5 PT/35 AT. *proL* tRNAs: Blue bars and *proK* tRNAs: Red bars.

compared to the $proK^{WT}$. Furthermore, ∼3–15% of the mutant proline tRNAs appeared to be polyadenylated (Figure 5B). Thus, ∼3% of $proL^{5M}$ tRNAs (1/30 cDNAs), and ∼ 15% of $proL^{5M+3M}$ (4/27 cDNAs), $proK^{5M}$ (4/26 cDNAs) and $proK^{5M+3M}$ (5/35 cDNAs) tRNAs with immature 3′ ends contained 1–7 untemplated A nucleotides (Figures 3C,D and 4C,D, upward arrow). Surprisingly, ∼12 ± 1% of the $proL^{5M}$ and $proL^{5M+3M}$ tRNAs sequenced were truncated either at the 5′ (*) or 3′ ends (downward solid arrow) (Figure 3C, D). Similarly, ∼23% of $proK^{5M}$ tRNAs (6/26 cDNAs) and ∼43% of of $proK^{5M+3M}$ tRNAs (15/35 cDNAs) were truncated by 5–24 nts at the 5′ end (Figure 4C,D, *).

Taken together, the sequencing results confirmed that the mutant proline tRNAs were accurately transcribed. However, the tRNAs were processed differently by both RNase E at the 3′ end and RNase P at the 5′ end compared to the wild type proline tRNAs. Thus, both 5′ modified *proL* and *proK* tRNAs had altered processing not only at the 3′-ends, but also at the 5′-ends and became substrates for poly(A) polymerase (Figures 3, 4 and 5B). Since the processing patterns of the 5′-modified proline tRNAs ($proL^{5M}$ and $proK^{5M}$ tRNAs) were very similar to those of both 5′ and 3′ modified proline tRNAs ($proL^{5M+3M}$ and $proK^{5M+3M}$ tRNAs), the data also suggested that the 5′-modification was primarily responsible for the change in the cleavage specificity of RNase E at the 3′ end.

The 5′ modified proline transcripts require 3′→ 5′ exonucleases for 3′ end maturation

The data presented in Figures 3 and 4 indicated that a significant fraction of the 5′ modified *proL* and *proK* transcripts retained at least 1–2 nts downstream of CCA, which would require 3′ → 5′ exonucleases for their final 3′-end maturation. Thus, we expected that the level of 5′ modified proline tRNAs with 3′-immature termini to increase substantially in a *Δrnt Δrph* double mutant.

Accordingly, we expressed all the proline plasmids in a *Δrnt Δrph* genetic background and analyzed the processing of the modified *proK* and *proL* tRNAs by northern blot analysis. As expected, <5% of the $proL^{WT}$ and $proL^{3M}$ (Figure 6A, lanes 1 and 3) as well as $proK^{WT}$ and $proK^{3M}$ (Figure 6B, lanes 1 and 2) tRNAs were larger than the mature tRNA in the *Δrnt Δrph* strains. In contrast, ∼ 50% of the $proL^{5M}$ (Figure 6A, lane 2) and $proK^{5M}$ (Figure 6B, lane 3) transcripts were a few nucleotides larger than the mature tRNA, an observation typical of tRNAs with immature 3′ ends in the exonuclease mutants (10). While a similar percentage of the $proK^{5M+3M}$ transcripts were immature (Figure 6B, lane 4), no significant accumulation of the immature tRNAs for the $proL^{5M+3M}$ transcripts was observed (Figure 6A, lane 4). It was likely that the immature $proL^{5M+3M}$ transcripts were rapidly degraded, since the amount of mature tRNA was significantly less than observed with the wild-type or any $proL^{3M}$ species (Figure 6, lanes 1, 3 and 4).

To provide further evidence that the $proL^{5M}$ and $proK^{5M}$ tRNAs contained unprocessed nucleotides downstream of the CCA determinant in the exonuclease mutant following initial RNase E cleavage, we determined the 5′ and 3′ termini of the mutant tRNAs. Thus, cDNAs generated following 5′-3′ self-ligation of the transcripts were cloned and sequenced as described in the Materials and Methods section. As expected, ∼76% (19/25 cDNAs) of the $proL^{5M}$ tRNAs retained 2–4 nucleotides downstream of CCA (Figure 7A). Similarly, ∼80% (20/25 cDNAs) of $proK^{5M}$ tRNA retained 2 nucleotides downstream of CCA (Figure 7B). Furthermore, ∼12–28% of both tRNAs contained untemplated A residues.

5′ modified proline tRNAs appear to be stable

To determine if the reduced steady-state levels of the 5′ modified *proL* and all the *proK* tRNAs (Figure 2) was due to their decreased stability, we attempted to determine their half-lives. Accordingly, northern blot analysis was carried

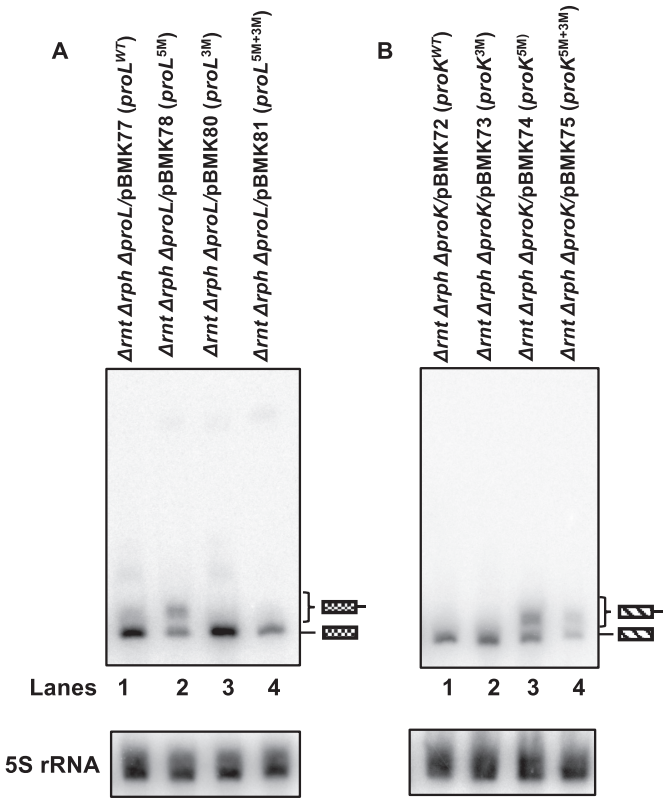

Figure 6. Northern blot analyses of the processing of *proL* and *proK* tRNAs expressed from various plasmids in the absence of RNase PH and RNase T. Total steady-state RNA (10 μg/lane) isolated from exponentially growing cultures at 37°C was separated on a 6% (w/v) acrylamide/ 8 M urea gel, transferred to nylon membrane, and probed with transcript specific ^{32}P-labelled oligonucleotide probes. Northern blots of (**A**) *proL* tRNA probed with probe a (Figure 2A) and (**B**) *proK* tRNA probed with probe b (Figure 2C). The genotypes of the strains used are indicated at the top of each blot. The position of the mature and immature tRNAs are indicated to the right of the blots. The northern blot of 5S rRNA used as a loading control is shown below each blot. The multiple bands of 5S rRNA are due to its dependence on RNase T for the final 3′-end maturation (35).

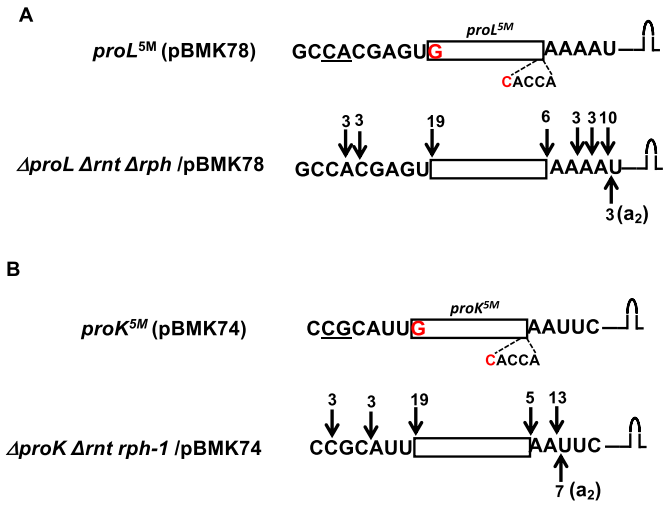

Figure 7. Determination of 5′ and 3′ termini of (**A**) *proL* (**B**) *proK* tRNAs expressed from various plasmids in the absence of RNase PH and RNase T. The cDNAs were obtained by RT-PCR cloning of 5′-3′ self-ligated transcripts. The cloned proline genes with the coding sequences upstream and downstream of the 5′ and 3′ ends, respectively, are shown at the top of each sequenced data and explained in the legends to Figures 3 and 4. Each downward arrow represents either 5′ or 3′ ends (total number indicated at the top) as determined by sequence analysis. Each upward arrow represents a 3′ end with untemplated A nucleotides (in parenthesis).

out using total RNAs isolated from various strains after blocking the new transcription with the addition of rifampicin. However, we were unable to determine the half-lives of the proline transcripts, since all the *proL* and *proK* transcript levels either kept increasing or remained similar for up to 90 min after the addition of the rifampicin (Supplementary Figure S4A, S4B).

As another control, we probed the blots for the *proM* transcript levels, which showed that they also remained unchanged in all the genetic backgrounds (Supplementary Figure S4A, S4B). To confirm that the rifampicin had blocked new transcription initiation we also probed the blot for the *lpp* mRNA. In this case, the *lpp* mRNA levels decreased as expected over time after the rifampicin addition, yielding half-lives in agreement with previously reported results (data not shown) (22–24).

An increase in the mature tRNA levels after the rifampicin addition has been previously reported (8,25). In fact, the increase in the levels of tRNAs and 5S rRNA over time following the addition of rifampicin in *E. coli* has been attributed to a 50% decrease in the total RNA arising primarily from significant decreases in 23S and 16S rRNAs (26).

The 5′-modified proline tRNAs are not aminoacylated

Since the steady-state levels of the 5′ modified proline tRNAs were reduced significantly (Figures 2 and 5), we wanted to determine the functionality of the modified mature tRNAs. Accordingly, we determined the *in vivo* aminoacylation levels of all the modified tRNAs using the method of Varshney *et al.* (21). With this technique aminoacylated tRNAs isolated under acidic conditions are distinguished from the uncharged tRNAs by their higher molecular weight when separated in an acid urea gel. Thus, equal amounts of total RNA isolated under acidic conditions, before and after treatment with Tris (which chemically deacylates the tRNAs), were separated in an acid urea polyacrylamide gel. No significant differences in the aminoacylation levels among the wild-type and 3′ modified *proL* (Figure 8A, lanes 1–4, 7–8) and *proK* (Figure 8B, lanes 1–6) tRNAs were observed. In striking contrast, both the 5′ as well as 5′ and 3′ modified *proL* (Figure 8A, lanes 5–6, 9–10) and *proK* tRNAs (Figure 8B, lanes 7–10) appeared to be either poorly or not aminoacylated at all, since the Tris treatment had no significant effect on the tRNA molecular weights. As a control, we also probed the blot for the *proM* tRNA, which showed identical aminoacylation levels in all the strains tested (Figure 8A,B, lanes 1–10).

Changing the *pheV* tRNA 5′-mature nucleotide G to C led to inviability

Since changing the C to G nucleotide in the *proL* and *proK* tRNAs 5′-mature end resulted in RNase E cleavage 1–2 nts

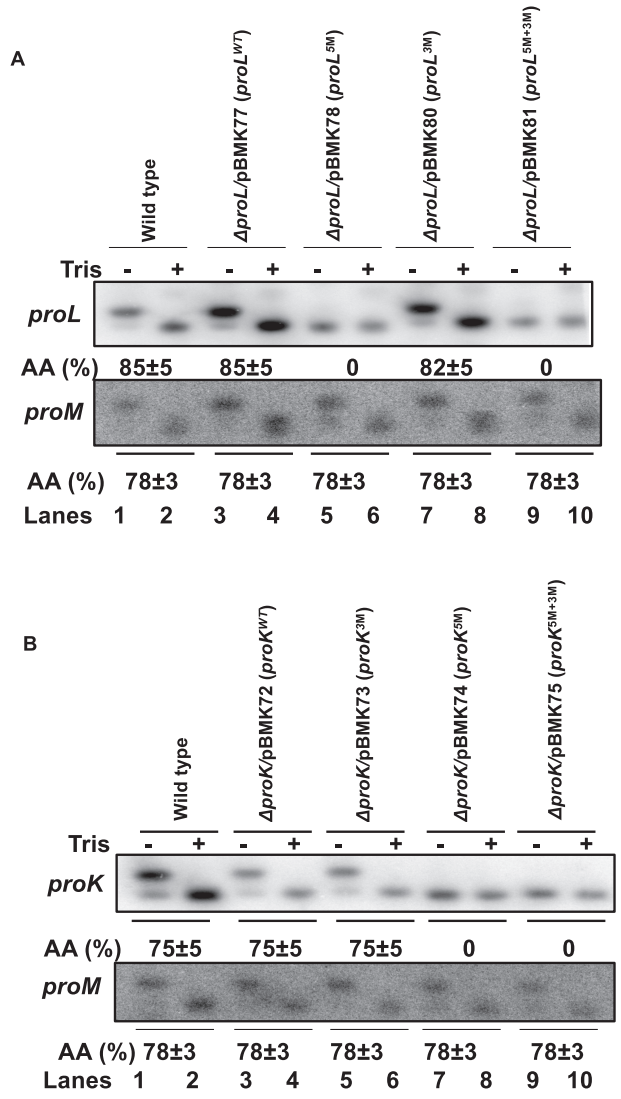

Figure 8. Determination of aminoacylation levels of (**A**) *proL* and (**B**) *proK* tRNA expressed from various plasmids by northern blot analysis. Total RNA isolated under acidic condition from various strains were either untreated (−) or treated (+) with 0.5 M Tris (pH 9) to chemically deacylate tRNAs and were separated using acid urea polyacrylamide gel (6.5%, w/v) as described in Materials and Methods section. The blot was probed with ^{32}P-end labeled oligo probe a for *proL* (Figure 2A) and probe b for *proK* (Figure 2C). Each blot was also probed with *proM* specific probe PROMS-2 (Supplementary Table S2) as a control. The genotypes of the strains used are indicated at the top of each blot. The level of aminoacylation (AA) for each tRNA was calculated as percentage of tRNAs deacylated after Tris treatment compared to total tRNAs before tris treatment (8) and represent the average of three independent determinations.

downstream of CCA (Figures 3, 4, 7), we hypothesized that changing the first nucleotide of a tRNA that contains G at the 5′-mature end to C would result in a RNase E cleavage at the mature 3′-end of the tRNA. We selected the phenylalanine (*phe*) tRNAs for this experiment, since there are only two *phe* genes (*pheV* and *pheU*), both of which are monocistronic, G is the first nucleotide at the mature 5′-end, and RNase E cleaves at 2–3 nt downstream of the CCA (16). Since the two *phe* tRNAs are identical in their mature sequences, we deleted both the chromosomally encoded *pheV* and *pheU* sequences and the double deletion mutant was kept alive with a covering plasmid carrying the wild-type *pheV* gene (pVMK208/$pheV^{WT}$) (see Materials and Methods).

Plasmids containing various *pheV* mutant coding sequences were generated similar to proline tRNA modifications (Table 1). Accordingly, the nucleotide sequences downstream of the CCA determinant were changed from CTAA to AATT (same as *proK*) in the 3′ modified *pheV* tRNA (pVMK210/$pheV^{3M}$). The G/C base pair at the 5′-mature terminus was changed to C/G base pair in the 5′ modified *pheV* tRNA (pVMK214/$pheV^{5M}$). Both the 3′ and 5′ modifications were combined in the 5′ and 3′ modified *pheV* tRNA (pVMK212/$pheV^{5M+3M}$). Subsequently, we attempted to displace the pVMK208/$pheV^{WT}$ with plasmids containing the mutant *pheV* sequences to study the processing of the mutant *pheV* tRNAs. The pVMK208/$pheV^{WT}$ was easily displaced by pVMK210/$pheV^{3M}$. However, neither the pVMK214/$pheV^{5M}$ nor the pVMK212/$pheV^{5M+3M}$ was able to displace pVMK208/$pheV^{WT}$. These data suggested that while changing the downstream sequences of *pheV* CCA had no effect on functionality of *pheV* tRNA, changing the G to C as the first nucleotide at the mature 5′-end most likely made the tRNA non-functional. The data were consistent with the results obtained with the modified *proL* and *proK* tRNAs except the strains containing 5′-modified proline tRNAs were viable due to presence of the genomic copy of the *proM*.

DISCUSSION

The data presented here demonstrate that C, the first residue at the mature 5′ terminus of the *proL* and *proK* tRNAs in *E. coli* is not only required for their 3′ maturation by the one step RNase E cleavage reaction but is also essential for their functionality. This conclusion is supported by the fact that wild-type tRNAs ($proL^{WT}$ and $proK^{WT}$) were processed at their mature 3′ ends (Figures 3A and 4A) in agreement with previous observations (10). In contrast, by changing the 5′ mature nucleotide of the *proL* and *proK* tRNAs from C to G, a nucleotide that is found at the 5′ mature termini of 67/86 of the other *E. coli* tRNAs, RNase E no longer cleaved immediately downstream of the CCA determinant. Instead, ∼57% of $proL^{5M}$ and ∼69% of $proK^{5M}$ transcripts were processed at least 1–4 nucleotides downstream of CCA in the wild type strain (Figures 3C and 4C). In contrast, changing the nucleotide sequences downstream of the CCA determinant to mimic either *hisR* or *cysT* (both of these tRNAs are cleaved 2–3 nts downstream of CCA by RNase E) did not change RNase E processing of either the $proL^{3M}$ or $proK^{3M}$ variants (Figures 3B and 4B). In addition, the 3′ processing of $proL^{5M+3M}$ and $proK^{5M+3M}$ tRNAs, where both the 5′ mature nucleotide and the 3′ downstream sequences were changed, looked similar to the $proL^{5M}$ and $proK^{5M}$ tRNAs (Figures 3D and 4D), suggesting that the 5′ nucleotide is responsible for the RNase E cleavage specificity at the 3′ end.

Furthermore, the level of both the 5′ modified proline pre-tRNAs, which retained 1–4 nts downstream of CCA increased to 80% in the *Δrnt Δrph* double mutant (Figures 6 and 7), suggesting the additional requirement for 3′

→ 5′ exonuclease (RNase T and RNase PH) activity for the final 3′-end maturation following the RNase E cleavage. In addition, up to ∼15% of the $proL^{5M}$ and $proK^{5M}$ pre-tRNAs were polyadenylated in the wild-type strain (Figure 5B), increasing up to ∼28% in the *Δrnt Δrph* double mutant (Figure 7). This result was consistent with our previous report that pre-tRNAs with at least one additional nucleotide downstream of the CCA require 3′ → 5′ exonucleases, specifically RNase T and RNase PH, for their final 3′-end maturation and undergo significant levels of polyadenylation in their absence (8).

Unexpectedly, the expression of *proL* and *proK* appeared to be different from the same 6–8 copy plasmids. While ∼5-fold increase in the $proL^{WT}$ expression compared to the genomic *proL* expression was consistent with the copy number of pBMK77, a ∼3-fold decrease in the $proK^{WT}$ expression from pBMK72 compared to the genomic *proK* expression was surprising (Figure 2B, D). Although an increase in the concentration of the chromosomally encoded tRNAs with the increase in their gene dosage has been reported (27), our data suggest that the same correlation may not apply when the tRNAs are expressed extra chromosomally. Since both tRNAs are very stable (Supplementary Figure S4), we speculate that transcriptional regulation of these tRNAs plays a role in their steady-state levels. It has been shown that the intracellular concentration of *proL* is almost twice that of the *proK* tRNA isotype and that the codon usage of the *proL* tRNA is almost 6–10 times higher than *proK* tRNA isotype in an exponentially growing cell (28). Thus, with the *proK* tRNA being less used compared to *proL* tRNA, it is possible that the steady-state level of *proK* tRNA is transcriptionally downregulated.

Another surprising observation was the occurrence of a spontaneous deletion mutation in the −35 element of the modified *proK* promoter sequences (Supplementary Figure S2) that resulted in either the reduction or abolition of the transcription of the 5′ modified *proK* tRNAs ($proK^{5M}$and $proK^{5M+3M}$). Previously, we have observed that the expression of the *pcnB* gene from the plasmid was effectively blocked by a single nucleotide change in the −35 region in order to avoid PAP I toxicity (29). However, the strains expressing the 5′-modified *proK* tRNAs ($proK^{5M}$and $proK^{5M+3M}$) did not appear to be under any kind of stress condition based on their identical growth rates compared to the wild-type strain (data not shown). In addition, while the expression of the 5′ modified *proL* tRNAs ($proL^{5M}$and $proL^{5M+3M}$) was also reduced (Figure 2B), no spontaneous mutations have been observed with these constructs.

While changing the C at the mature 5′-end of proline tRNAs to the more prevalent G nucleotide maintained the Watson-Crick base pair in the acceptor stem, the modified tRNA could not be aminoacylated (Figure 8), which might have also contributed to their lower steady-state levels (Figure 2). It should be noted that ∼40% of the 5′ modified proline tRNAs were immature at the 5′ end and ∼70% were immature at the 3′-end (Figures 3 and 4), which might be partially responsible for the loss in aminoacylation. While the aminoacylation of the 5′ immature proline tRNAs (with <8 unprocessed nucleotides) was expected to occur (9), only tRNAs with the 3′ immature termini were not expected to be aminoacylated. However, the absence of any aminoacylation of the 5′-modified proline tRNAs, even though up to ∼40% of these tRNAs were matured (Figure 5A), suggested involvement of additional factors.

In fact, the N1-N72 base pair together with the discriminator base at N73 have been shown to play the role of determinant or antideterminant for the recognition of the tRNAs by several enzymes that includes a majority of the aminoacyl-tRNA synthetases. Specifically, G72 and A73 serve as the major determinant/recognition element for *E. coli* prolyl-tRNA synthetase (ProRS) and a substitution at G72 to C72 led to 31-fold decrease in aminoacylation *in vitro* (30). Thus, the complete failure of the aminoacylation of the 5′-modified proline tRNAs is most likely the result of the change in the one of the recognition elements (G72→C72) for ProRS which in turn is directly related to the change from C1 to G1. The failure of the aminoacylation of both $proL^{5M}$ and $proK^{5M}$ mature tRNAs (Figure 8A,B) is the first *in vivo* demonstration of the consequences of the modifications to the first nucleotide of the proline tRNAs and is consistent with the *in vitro* study (30).

Although we would have liked to study the processing of the 5′-modified *proM* tRNA in the similar fashion, we were unable to delete the genomic copy of the gene suggesting it is essential. In fact, although the *proM* tRNA recognizes the CCA, CCU and CCG codons, only the CCU and CCG codons are recognized by the *proK* and *proL,* respectively. Thus, the inability to read the CCA codon by either *proL* or *proK* tRNA isotype is probably the reason why *proM* is an essential gene. However, since the *proM* contains the same C1/G72 base pair in its acceptor stem and undergoes the 3′-end maturation by one-step RNase E cleavage utilizing the same processing pathway as that of *proK* and *proL* tRNAs (10), it is reasonable to expect that the C nucleotide at the mature 5′ end of all three proline tRNAs is indispensable.

The data presented above raise an important question regarding the significance of C as the first nucleotide at the mature 5′-end of the proline tRNAs. However, our data can also be explained based on the N1-N72 base pair, which is one of the highly conserved nucleotide pairs in all tRNA isotypes found in bacteria but is less conserved in eukarya (17,31). Specifically, C1-G72 base pair in proline tRNAs is highly conserved in all bacteria in contrast to archaea and eukaryotes, which contain a G1-C72 base pair (17). In fact, it is believed that the recognition of proline tRNA by ProRS has changed through evolution where functional coadaptations have occurred from the bacteria to the human enzymes (32).

In the case of *pheV* tRNA, by changing the nucleotide at the mature 5′-end from G to C ($pheV^{5M}$) with the expectation of direct RNase E cleavage at the mature 3′-end of *pheV* CCA, the $pheV^{5M}$ tRNA most likely could not be aminoacylated and therefore could not support cell viability. Unlike the nonfunctional $proL^{5M}$ and $proK^{5M}$ tRNAs, where a genomic copy of a functional *proM* tRNA (Figure 8A,B) can complement the loss of both *proL* and *proK* tRNA and is sufficient to support cell viability, in the case of the $pheV^{5M}$ variant, the *pheU* isotype tRNA is deleted and there is not another isotype to complement the loss.

Taken together, the above data clearly demonstrated that the first nucleotide (N1) at the mature 5′ end of a tRNA is critical for its functionality. Since N1/N72 base pairing is conserved for all elongator tRNAs (17), C1/G72 base pairing in proline tRNAs is required not only for its maturation, but for the aminoacylation of the matured tRNA. It should also be noted that an extra 5′-nucleotide (G-1) in the $tRNA^{His}$ has been shown *in vitro* to be essential for its aminoacylation (33,34). Thus, the interaction of a specific tRNA with its cognate aminoacyl tRNA synthetase, which has evolved over time, may hold the key to the specificity of a nucleotide at the mature 5′-end of a tRNA (31).

SUPPLEMENTARY DATA

Supplementary Data are available at NAR Online.

FUNDING

National Institutes of Health (NIH) [GM81544 to S.R.K.]. Funding for open access charge: NIH [GM81544].
Conflict of interest statement. None declared.

REFERENCES

1. Mohanty,B.K. and Kushner,S.R. (2019) New insights into the relationship between tRNA processing and polyadenylation in *Escherichia coli*. *Trends Genet.*, **35**, 434–445.
2. Li,Z. and Deutscher,M.P. (2002) RNase E plays an essential role in the maturation of *Escherichia coli* tRNA precursors. *RNA*, **8**, 97–109.
3. Ow,M.C. and Kushner,S.R. (2002) Initiation of tRNA maturation by RNase E is essential for cell viability in *E. coli*. *Genes Dev.*, **16**, 1102–1115.
4. Mohanty,B.K. and Kushner,S.R. (2007) Ribonuclease P processes polycistronic tRNA transcripts in *Escherichia coli* independent of ribonuclease E. *Nucleic Acids Res.*, **35**, 7614–7625.
5. Mohanty,B.K. and Kushner,S.R. (2008) Rho-independent transcription terminators inhibit RNase P processing of the *secG leuU* and *metT* tRNA polycistronic transcripts in *Escherichia coli*. *Nucleic Acids Res.*, **36**, 364–375.
6. Agrawal,A., Mohanty,B.K. and Kushner,S.R. (2014) Processing of the seven valine tRNAs in *Escherichia coli* involves novel features of RNase P. *Nucleic Acids Res.*, **42**, 11166–11179.
7. Mohanty,B.K. and Kushner,S.R. (2010) Processing of the *Escherichia coli leuX* tRNA transcript, encoding $tRNA^{leu5}$, requires either the 3′−5′ exoribonuclease polynucleotide phosphorylase or RNase P to remove the Rho-independent transcription terminator. *Nucleic Acids Res.*, **38**, 597–607.
8. Mohanty,B.K., Maples,V.F. and Kushner,S.R. (2012) Polyadenylation helps regulate functional tRNA levels in *Escherichia coli*. *Nucleic Acids Res.*, **40**, 4589–4603.
9. Mohanty,B.K., Agrawal,A. and Kushner,S.R. (2020) Generation of pre-tRNAs from polycistronic operons is the essential function of RNase P in *Escherichia coli*. *Nucleic Acids Res.*, **48**,2564–2578.
10. Mohanty,B.K., Petree,J.R. and Kushner,S.R. (2016) Endonucleolytic cleavages by RNase E generate the mature 3′ termini of the three proline tRNAs in *Escherichia coli*. *Nucleic Acids Res.*, **44**, 6350–6362.
11. Chao,Y., Li,L., Girodat,D., Forstner,K.U., Said,N., Corcoran,C., Smiga,M., Papenfort,K., Reinhardt,R., Wieden,H.J. *et al.* (2017) *In vivo* cleavage map illuminates the central role of RNase E in coding and non-coding RNA pathways. *Mol. Cell*, **65**, 39–51.
12. Jourdan,S.S., Kime,L. and McDowall,K.J. (2010) The sequence of sites recognised by a member of the RNase E/G family can control the maximal rate of cleavage, while a 5′-monophosphorylated end appears to function cooperatively in mediating RNA binding. *Biochem. Biophys. Res. Comm.*, **391**, 879–883.
13. Kaberdin,V.R. (2003) Probing the substrate specificity of *Escherichia coli* RNase E using a novel oligonucleotide-based assay. *Nucleic Acids Res.*, **31**, 4710–4716.
14. McDowall,K.J., Kaberdin,V.R., Wu,S.-W., Cohen,S.N. and Lin-Chao,S. (1995) Site-specific RNase E cleavage of oligonucleotides and inhibition by stem-loops. *Nature*, **374**, 287–290.
15. Li,Z., Gong,X., Joshi,V.H. and Li,M. (2005) Co-evolution of tRNA 3′ trailer sequences with 3′ processing enzymes in bacteria. *RNA*, **11**, 567–577.
16. Bowden,K.E., Wiese,N.S., Perwez,T., Mohanty,B.K. and Kushner,S.R. (2017) The *rph-1*-encoded truncated RNase PH protein inhibits RNase P maturation of Pre-tRNAs with short leader sequences in the absence of RppH. *J. Bacteriol.*, **199**, e00301-17.
17. Marck,C. and Grosjean,H. (2002) tRNomics: Analysis of tRNA genes from 50 genomes of Eukarya, Archaea, and Bacteria reveals anticodon-sparing strategies and domain-specific features. *RNA*, **8**, 1189–1232.
18. Datsenko,K.A. and Wanner,B.A. (2000) One-step inactivation of chromosomal genes in *Escherichia coli* K-12 using PCR products. *Proc. Natl. Acad. Sci. USA*, **97**, 6640–6645.
19. Wang,R.F. and Kushner,S.R. (1991) Construction of versatile low-copy-number vectors for cloning, sequencing and gene expression in *Escherichia coli*. *Gene*, **100**, 195–199.
20. Mohanty,B.K. and Kushner,S.R. (2019) Analysis of post-transcriptional RNA metabolism in prokaryotes. *Methods*, **155**, 124–130.
21. Varshney,U., Lee,C.P. and RajBhandary,U.L. (1991) Direct analysis of aminoacylation levels of tRNAs *in vivo*. Application to studying recognition of *Escherichia coli* initiator tRNA mutants by glutaminyl-tRNA synthetase. *J. Biol. Chem.*, **266**, 24712–24718.
22. Mohanty,B.K. and Kushner,S.R. (1999) Analysis of the function of *Escherichia coli* poly(A) polymerase I in RNA metabolism. *Mol. Microbiol.*, **34**, 1094–1108.
23. Mohanty,B.K. and Kushner,S.R. (2003) Genomic analysis in *Escherichia coli* demonstrates differential roles for polynucleotide phosphorylase and RNase II in mRNA abundance and decay. *Mol. Microbiol.*, **50**, 645–658.
24. O'Hara,E.B., Chekanova,J.A., Ingle,C.A., Kushner,Z.R., Peters,E. and Kushner,S.R. (1995) Polyadenylylation helps regulate mRNA decay in *Escherichia coli*. *Proc. Natl. Acad. Sci. U.S.A.*, **92**, 1807–1811.
25. Dittmar,K.A., Mobley,E.M., Radek,A.J. and Pan,T. (2004) Exploring the regulation of tRNA distribution on the genomic scale. *J. Mol. Biol.*, **337**, 31–47.
26. Hamouche,L., Poljak,L. and Carpousis,A.J. (2021) Ribosomal RNA degradation induced by the bacterial RNA polymerase inhibitor rifampicin. *RNA*, **27**, 946–958.
27. Komine,Y., Adachi,T., Inokuchi,H. and Ozeki,H. (1990) Genomic organization and physical mapping of the transfer RNA genes in Escherichia coli K12. *J. Mol. Biol.*, **212**, 579–598.
28. Dong,H., Nilsson,L. and Kurland,C.G. (1996) Co-variation of tRNA abundance and codon usage in *Escherichia coli* at different growth rates. *J. Mol. Biol.*, **260**, 649–663.
29. Mohanty,B.K. and Kushner,S.R. (2013) Deregulation of poly(A) polymerase I in *Escherichia coli* inhibits protein synthesis and leads to cell death. *Nucleic Acids Res.*, **41**, 1757–1766.
30. Liu,H., Peterson,R., Kessler,J. and Musier-Forsyth,K. (1995) Molecular recognition of tRNA(Pro) by Escherichia coli proline tRNA synthetase in vitro. *Nucleic Acids Res.*, **23**, 165–169.
31. Tamaki,S., Tomita,M., Suzuki,H. and Kanai,A. (2018) Systematic analysis of the binding surfaces between tRNAs and their respective aminoacyl tRNA synthetase based on structural and evolutionary data. *Front. Genet.*, **8**, 227.
32. Stehlin,C., Burke,B., Yang,F., Liu,H., Shiba,K. and Musier-Forsyth,K. (1998) Species-specific differences in the operational RNA code for aminoacylation of tRNAPro. *Biochemistry*, **37**, 8605–8613.
33. Seetharaman,M., Williams,C., Cramer,C.J. and Musier-Forsyth,K. (2003) Effect of G-1 on histidine tRNA microhelix conformation. *Nucleic Acids Res.*, **31**, 7311–7321.
34. Himeno,H., Hasegawa,T., Ueda,T., Watanabe,K., Miura,K. and Shimizu,M. (1989) Role of the extra G-C pair at the end of the acceptor stem of tRNA(His) in aminoacylation. *Nucleic Acids Res.*, **17**, 7855–7863.
35. Li,Z. and Deutscher,M.P. (1995) The tRNA processing enzyme RNase T is essential for maturation of 5S RNA. *Proc. Natl. Acad. Sci. USA*, **92**, 6883–6886.